Presented at the 11th International Conference on
Magnet Technology, Tsukuba, Japan,
August 28-September 1, 1989

SSC-N-665

MEASUREMENTS OF QUENCH PROPAGATION VELOCITY ALONG A SUPER-STABILIZED CONDUCTOR*

A. Devred
SSC Central Design Group†
c/o Lawrence Berkeley Laboratory
One Cyclotron Road, MS 90-4040
Berkeley, CA 94720 USA

ABSTRACT

The transition of a superstabilized conductor to the normal resistive state is accompanied by a redistribution of current which, due to the size of the normal metal matrix, is long compared with the thermal propagation and greatly affects the propagation velocity. To simulate adiabatic propagation, a 2-m sample of ALEPH conductor, suspended in a vacuum and indirectly cooled at its extremities, was tested. Quenches were induced by heaters, and velocities were measured using voltage taps. Results are presented of tests at different currents and under different magnetic fields. These results are in good agreement with theoretical predictions.

INTRODUCTION

In composite, multifilament conventional superconductors, normal zone propagation is a strictly thermal phenomenon. It occurs close to the transition front, where a fraction of the power dissipated in the normal zone is transmitted by conduction to the superconducting zone, which in turn heats up and goes into transition. In superstabilized superconductors, like that developed for the ALEPH solenoid[1] where a conventional composite is enclosed in a large section of aluminum, an electromagnetic diffusion phenomenon is added. Indeed, close to the transition front, the current previously carried by the filaments is expelled toward the copper of the composite and toward the aluminum. Given the large section of the aluminum, the current needs a certain amount of time and space to diffuse itself. The transition front thus leaves a wake of electromagnetic diffusion, along which the dissipated power density per unit volume progressively decreases.

The question then arises of how the current redistribution affects the propagation velocity. In previous papers[2,3,4] we have developed a theoretical model for the propagation of the normal zone along a layer of superstabilized conductors representative of the ALEPH solenoid shown in Figure 1. In this indirect cooling configuration, the annular ring and the layer insulation introduce a high thermal resistance between the helium and the conductors. Our model therefore assumes that, at the scale of the propagation phenomenon, the amount of heat transferred to the helium is negligible and thus that the layer of conductors can be considered adiabatic. Treating the composite material as a homogeneous medium, and assuming that the current diffusion through the copper of the composite is instantaneous at the

*This work is part of a Ph.D. thesis completed at the Commissariat à l'Energie aAtomique, CEN/Saclay, DPhPE/STIPE/STCM, 91191 Gif-sur-Yvette cédex (France)

†Operated by Universities Research Association, Inc., for the U.S. Department of Energy.

scale of the diffusion through the aluminium, we solve the equations of electromagnetic behavior and establish a general formula for the velocity. Reference 5 provides a summary of our theoretical results.

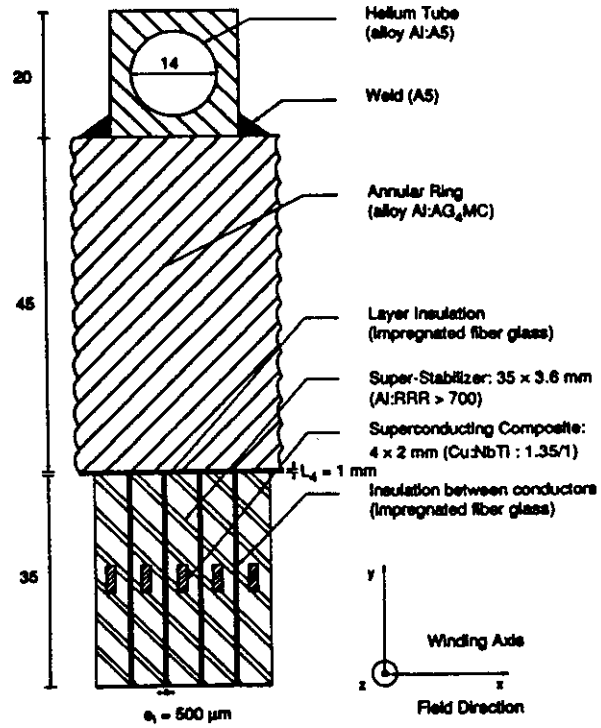

Figure 1. Cut away view of the ALEPH solenoid.

This paper reports the results of the experimental tests of our analytical formula. So far, propagation velocities along superstabilized conductors have only been measured in helium bath[6] or in a 1-m bore model solenoid where the transverse effects predominate.[7] Our goal was to recreate as closely as possible the assumptions of our theoretical model. Among them are (1) a constant-velocity propagation mode and (2) the hypothesis of adiabaticity. To be able to demonstrate the existence of a constant propagation velocity, we considered a 2-m-long sample of ALEPH conductor. To simulate adiabatic behavior, we operated the sample in a vacuum and reduced as much as possible the thermal contact between the conductor and the mechanical supports. The whole test setup was placed inside a large superconducting coil to be able to generate on the sample a magnetic field comparable to the one seen by the conductor in the real solenoid. The quenches were induced by heaters, and the propagation was monitored by voltage taps and temperature sensors regularly spaced along the sample.

Three kinds of influences were studied: the operating current, the external magnetic field, and the initial energy deposition. While the current and the field dramatically affect the velocity, the amount of energy put into the heater to induce the quench does not influence the subsequent propagation. As expected, the propagation velocity does not depend on the initial conditions. In the following, we limit our presentation to the first two influences.

DESCRIPTION OF THE EXPERIMENTAL SET UP

To constrain the magnetic forces, the conductor sample is wound around a stainless-steel mandrel of external diameter 0.72 m (determined by the bore of the external coil) and fastened by seven epoxy staples. Two layers of Kapton (each 2-mm thick) insulate the conductor from the mandrel. The question is now what is the thermal coupling between the conductor, the Kapton, and the mandrel, and does it influence the propagation velocity? When the external field is nil, the conductor loop tends to expand in its own field, only held by the staples; we then expect the conductor to behave adiabatically. Under an external magnetic field, the circulation of the currents in the external coil and in the sample have been designed so that the conductor loop contracts onto the mandrel. In such cases, it is more likely that part or all of the Kapton will be involved in the propagation process. For the mandrel, however, temperature sensors located in holes drilled at its periphery record no variation during quench testing. Adding this observation to the fact that it takes more than 100 hours to cool down the mandrel, while the conductor is cold in less than 50 hours, we conclude that the thermal resistance between the conductor and the mandrel is high enough to be considered as infinite at the scale of the propagation.

The sample is cooled by thermal conduction along the conductor using two helium exchangers. The location and the mounting of these exchangers are shown in Figure 2. Each consists of a copper tube (10 mm i.d., 12 mm o.d.), brazed on a 20-cm-long and 3-cm-thick copper plate. The copper plate is soldered on the previously tinned conductor. At both extremities of the sample, bending considerations have made it necessary to remove the aluminum from the conductor. The conductor is then soldered on a 2-cm-thick copper plate, which plays the role of stabilizer and improves the heat

transfer between the sample and the exchangers (one extremity also includes a splice between composites). To avoid circulation of current through the helium pipes and to ensure electrical insulation to ground, insulating sleeves have been installed at appropriate locations in the refrigeration circuit. The mandrel has no specific refrigeration and only cools down through its weak thermal coupling to the conductor. The whole setup is surrounded by a shield at 20 K.

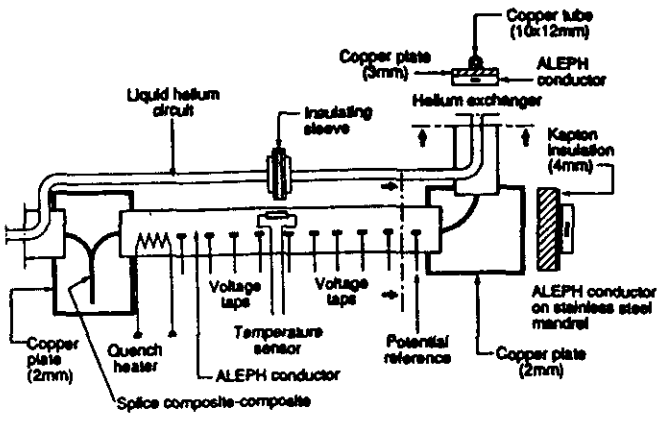

Figure 2. Experimental setup for measuring the propagation velocity along a sample of ALEPH conductor.

During testing, the operating pressure is regulated to 1.2 10^{-5} Pa corresponding to helium temperature of 4.4 K. Nevertheless, the sample temperature stabilizes around 5.1 K, 0.7 degrees higher than the cold source. This indicates residual thermal contributions, which can be estimated to be around 70 mK.[8] We have not been able to identify the origin of these residual thermal contributions, but we can verify that their influence on the velocity measurements is negligible. Indeed, we can bracket the temperature gradient induced along the sample by such thermal contributions. An upper limit is set by assuming that the 70 mK are punctually received in the middle of the sample, which leads to a gradient of 0.3 K. A lower limit is determined by assuming that the power is uniformly received along the sample, which leads to a value of 0.15 K. The temperature profiles corresponding to these gradients are very flat and thus should not invalidate our measurements.

As shown in Figure 2, the sample is equipped with a spot-heater, temperature sensors, and voltage taps. The heater, located at one extremity of the sample, consists of a flat bifilar coil (38 × 30 mm^2), wound with constantan wire, and glued to the conductor with Eccobond. The heater resistance is 38.4 Ω and hardly depends on the temperature. The temperature sensors are calibrated Allen Bradley resistors, which have been chosen for their high sensitivity at low temperatures and their stability under low magnetic fields.[9] In order to decrease the response time, the carbon insulation of the sensors is filed to bare the active piece (graphite). The active piece is then inserted and glued with Eccobond into a copper sleeve, which is soldered with indium on the conductor. The response time has been measured to be of the order of 1 millisecond.[8] There are ten voltage taps regularly spaced along the sample (one every 20 cm) 1.2 cm from the superior edge of the conductor. The voltage taps consist of a copper wire threaded into a counter bore (2-mm diameter, 3-mm deep) that has been drilled into the aluminium. The wire is held in position by a brass screw soldered with tin. Each bore is threaded with one wire, except the bore located at the sample extremity opposite the heater, which has been chosen as the reference for the voltage, and has nine wires. These nine wires are each paired with one of the other wires; the twisted pairs go into differential amplifiers. In the following, we only consider four voltage taps and one temperature sensor. Their locations reckoned from the reference tap are 341 mm, 744 mm,1046 mm, and 1250 mm for the taps; 1345 mm for the sensor. The taps are numbered starting with the one opposite the reference.

The external field is created by a superconducting magnet with a 1-m bore, equipped with an internal cryostat. The cryogenic circuits for the magnet and the sample are dissociated. The vacuum in the internal cryostat is maintained around 10^{-4} Pa.

TEST RESULTS

Unexpected behavior of the sample temperature appeared during testing. As we said, when the current is nil, the conductor temperature T_s stabilizes around 5.1 K. During the ramping of the current, eddy currents are induced in the stabilizer, which overheat the conductor. They disappear once a constant current has been established; the conductor then cools off and stabilizes again at a constant temperature. However, this constant temperature is higher than 5.1 K, increasing linearly with the current squared. The slope of the temperature increase also depends on the external field B_e. Expressions for $T_s = f(I)$ can be found in Table 1. This shows the existence of additional heating, presumably of Joule origin. An evaluation

of the resistance R_J producing this heating is given by

$$R_J = \frac{T_s(I) - T_s(I=0)}{R_{th} I^2},$$

where I is the current and R_{th} is the thermal resistance between the conductor and the exchangers. From the geometry of the exchangers, R_{th} can be evaluated around 10 K/W. The slope of T_s versus I when $B_e = 0$, then gives

$$R_J = 4.1\ 10^{-9}\ \Omega.$$

This value is typical of a weld between superconductors. We then conclude that the additional heat is generated in the splice located at the extremity of our sample (see Figure 2). The fact that the initial temperature of the sample is higher than expected is not a problem, since we can measure it. Of course, our comparison between experimental data and theoretical calculations will rely on these measured temperatures.

TABLE 1.
Selected Parameters for the Analytical Calculations

Critical temperatures (K)
$T_C = 9.5 - 0.5\,B$
$T_{CI} = 9.5 - 0.5\left(B + \frac{1+(0.9-0.09B)B}{2435} I\right)$
Field on the sample (T)
$B_{max} = B_e + 10^{-4} I \quad B_{av} = B_e + 5\ 10^{-5} I$
Sample temperature (K)
$T_s(0\ T) = 5.1 + 2.4\ 10^{-8} I^2$
$T_s(1\ T) = 5.3 + 4.3\ 10^{-8} I^2$
$T_s(1.55\ T) = 5.55 + 2.8\ 10^{-8} I^2$
$T_s(2.1\ T) = 5.25 + 4.75\ 10^{-8} I^2$

Figures 3a and 3b feature typical records of a voltage channel (channel 1) and of the nearby temperature sensor. The current at quench is 2500 A, and the external field is nil. The heater is fired at $t_0 = 375$ ms, and the pulse lasts $\tau_h = 100$ ms. The temporal evolution of the voltage can clearly be divided into four phases that are delimited on Figure 3a: (1) For $t \le t_1$, the voltage is nil; the quench has not yet reached tap 1, and the conductor between tap 1 and the reference tap is still superconducting. (2) For $t_1 \le t \le t_2$, the voltage rises rapidly; the quench has now reached tap 1 and propagates towards the reference tap. (3) For $t_2 \le t \le t_3$, the voltage decreases progressively; the whole conductor has now switched to the normal resistive state, but the current has yet to complete its redistribution through the superstabilizer, causing the decay of the apparent resistance. (4) For $t \ge t_3$, the voltage starts to rise again, but very slowly; the current is now redistributed, but as a result of the Joule heating the aluminum resistivity increases, causing the increase in the apparent resistance.

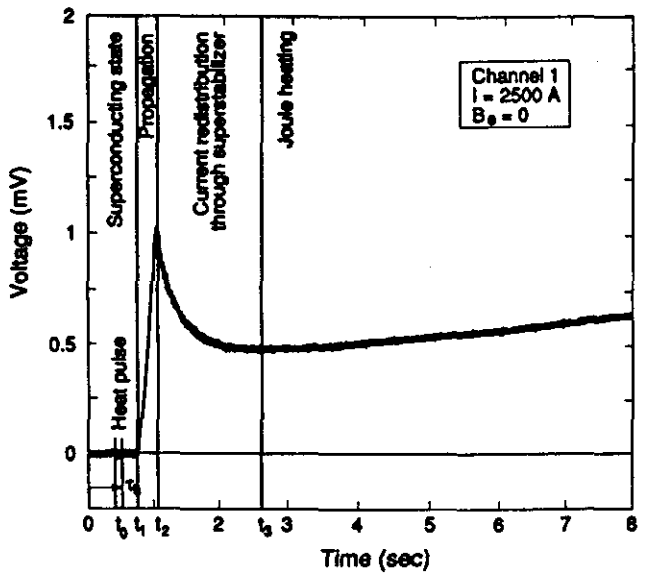

Figure 3a. Typical voltage evolution during a quench induced at 2500 A ($B_e = 0$ T).

These different phases can be correlated with the temporal evolution of the temperature shown in Figure 3b. For instance, at $t = t_1$, the temperature is about 9 K, which corresponds to the transition temperature of the conductor at 2500 A and thus correlates with the passage of the transition front near tap 1. Also, at $t = t_3$, the temperature is about 15 K, which, for the given purity of aluminum, corresponds to the end of the residual resistivity plateau; for temperatures greater than 15 K, the sample resistance thus increases.

From these data we conclude that thermal propagation is fast compared with electromagnetic diffusion, as predicted by the model. One can even verify that the times t_2 and t_3 are coherent with the characteristic times defined in Ref. 4 for these two phenomena.

To illustrate how the propagation velocity is determined, consider Figure 4. The current at quench is 1115 A, and the external field is nil. The four traces correspond to the voltages

between the reference tap and the four taps mentioned earlier. They rise in sequence. As expected, the quench, initiated at one extremity by the heater, gently propagates along the sample successively hitting the different taps. The velocity is simply measured by dividing the length between two successive taps by the difference in time between the takeoffs of the two voltages. The four voltage traces allow three different velocity measurements and thus enable us to see its evolution along the sample. It appears that the velocities measured between taps 1 and 2 are systematically 15 to 20 percent lower than the velocities measured between taps 2 and 3 and between taps 3 and 4, which are consistent. We are not able to explain this discrepancy. The sample does not indicate any obvious damage between taps 1 and 2. If the constant-velocity propagation mode had not been reached, we would expect the velocity to increase over each of the three lengths of conductor. Considering that the off-value is measured along 20.4 cm of conductor, when the two velocities in agreement are measured along lengths of 30.2 cm and 40.3 cm, we decided, in the following, to only retain these two values. Figure 5 shows a summary plot of these velocities versus the current at quench for all the tests run in a nil external field. The data points lie on the same curve with a small dispersion.

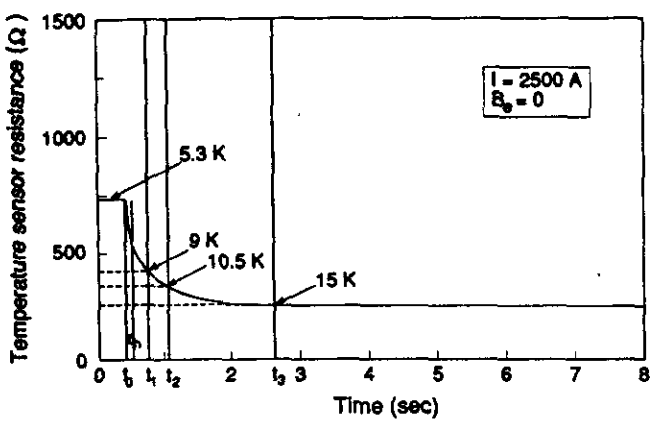

Figure 3b. Typical temperature evolution during a quench induced at 2500 A (B_e = 0 T).

Tests have been run for four external field values: 0 T, 1 T, 1.55 T, and 2.1 T. For each field value, the current in the sample was progressively increased from 1000 A to the critical current, in increments of 500 A. Each run, which provides two velocity measurements, was systematically doubled. This gives us about four hundred data points. The data are summarized in Figure 6 as a function of the current; the size of the plotting symbols represents the error bar. As in Figure 5, and for each field value, the data points lie on the same gentle curve.

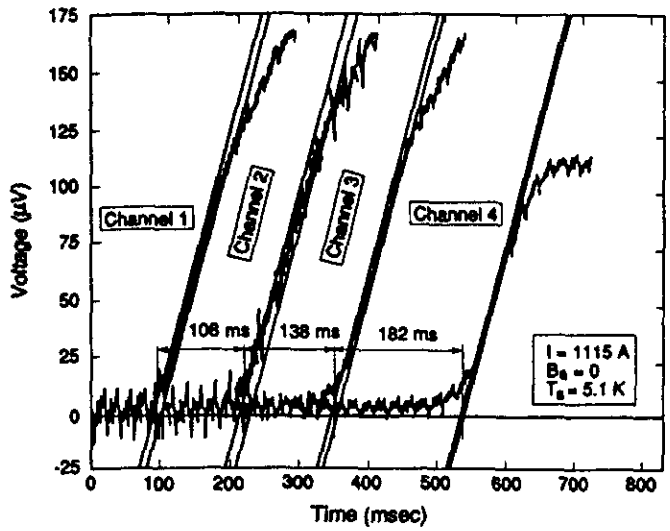

Figure 4. Example of determination of the propagation velocity for a quench induced at 1115 A (B_e = 0 T).

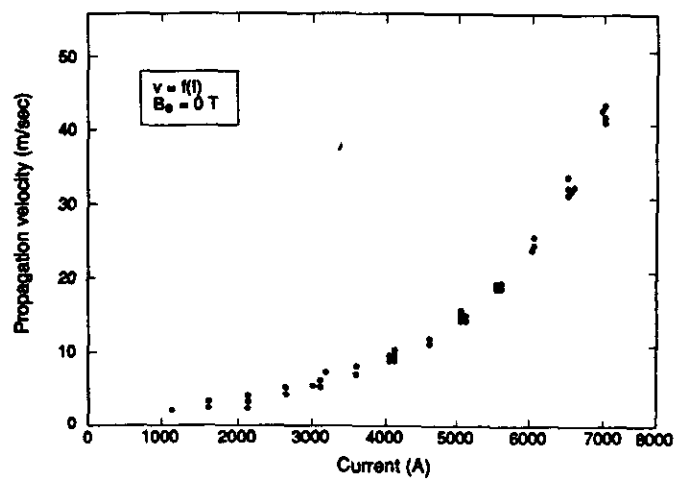

Figure 5. Summary plot of the velocity measurements (B_e = 0 T).

COMPARISON BETWEEN THEORY AND EXPERIMENT

The last step of our study is to compare the experimental data with the theoretical predictions. The details of our analytical formula can be found in Ref. 5. We nevertheless need to specify the

geometrical and physical characteristics we use in our calculation. The overall size of the superstabilized conductor is 34.15 × 3.45 mm^2. The composite is a 14-strand cable 5.75 × 1.36 mm^2. The strand diameter is 0.8 mm; the copper-to-superconductor ratio is 1.8 to 1. The copper and aluminum residual resistivity ratios are respectively 200 and 2200. Critical current measurements have been made at 4.2 K on six strands cut from the same conductor used in the experiment. The parametrization of T_{CI} given in Table 1 has been established assuming that the critical current is a linear function of the temperature. Also in Table 1 are formulas for the peak field, B_{max}, and the average field, B_{av}, on the conductor. The external field is given by the transfer function of the external coil; the own field is computed numerically. At a given current, the critical temperatures are calculated using the peak value, while the resistivities and the thermal conductivities of the materials are calculated using the average value. Lastly, the table shows linear approximations of $T_s = f(I)$ for the four values of B_e.

An obvious verification before analyzing the data of Figure 7 is to compare the critical currents actually measured in the experiment with the short sample predictions. For a given external field value, the short-sample current is the solution of the implicit equation

$$T_{CI}[I, B_{max}(I)] = T_s(I).$$

As shown in Table 2, these values are in good agreement.

With more confidence in our material properties, we turn to velocities. The data in Figure 6 show that for low currents, the values measured under external field are lower than the values without field. This is unexpected since T_C, T_{CI}, and the enthalpy per unit volume are decreasing functions of the magnetic field; the velocity should thus increase. (This is in fact the case when velocities under field are compared.) So, something, under the effect of the field, must slow down the propagation. One explanation is that, when the external field is nil, the conductor loop tends to expand under its own field, so that the thermal contact between the conductor and the Kapton insulation is poor, while under an external field, the loop contracts onto the mandrel, so that the contact between the conductor and the Kapton is greatly improved. This leads us to conclude that, in the absence of magnetic field, the Kapton does not interfere with the propagation process; under an external field, part or all of it is involved. In our analytical calculations, we then consider the conductor as bare in the absence of external field, but associated with the 4 mm of Kapton in the presence of field. Computation results are also plotted in Figure 6. Predictions and measurements appear in good agreement.

TABLE 2.
Comparison Between Predicted and Measured Critical Currents

B_{max} (T)	Predicted Critical Current (A)	Measured Critical Current (A)
0	7750	7500
1	6050	6000
1.55	5300	5100
2.1	4700	4500

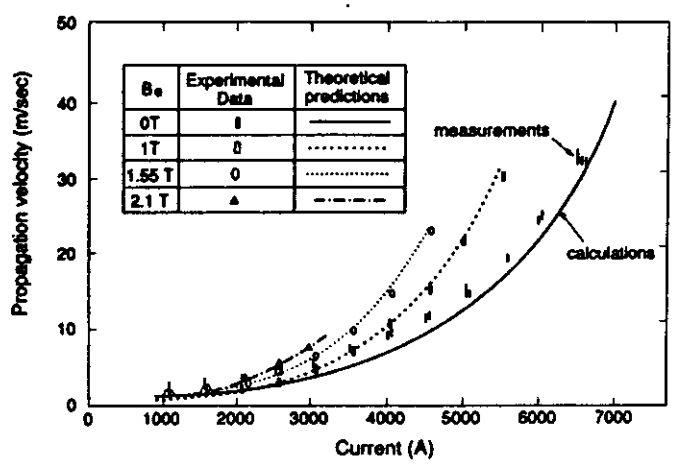

Figure 6. Comparison between predictions and measurements.

CONCLUSION

We have experimentally demonstrated the existence of a constant propagation velocity of the normal zone along superstabilized conductors, and we have verified that this velocity is in accord with the analytical law we had previously established. Our model of the current redistribution through the superstabilizer is thus justified. The next step towards a complete understanding of the quenching of the ALEPH solenoid would now be to investigate the transverse propagation.

ACKNOWLEDGMENTS

I am particularly grateful to the staff of the Sevice Technique de Cryogénie et de Magnétisme du CEN Saclay, whose skill and hard work made these tests possible. I want also to thank Katharine Metropolis for her comments on the manuscript, and Donna Matthews and Annie Calinog for their help in editing the text and preparing the figures.

REFERENCES

1. Desportes, H., LeBars, J., and Meuris, C., General design and conductor study for the ALEPH superconducting solenoid. (Proceedings of the 8th International Conference on Magnet Technology), J. Phys. (Paris), 1984, Colloque-45, C1–341.
2. Devred, A. and Meuris, C., Analytical solution for the propagation velocity of the normal zone in large matrix super-stabilized superconductor., (Proceedings of the 8th International Conference on Magnet Technology), J. Phys. (Paris), 1984, Colloque-45, C1-341.
3. Devred, A., Investigation of current redistribution in superstabilized superconducting winding when switching to the normal resistive state. J. Appl. Phys., 1989, **65** (10), 3963.
4. Devred, A., Investigation of the normal zone along a superstabilized superconducting solenoid. J. Appl. Phys. (September 1989, in press).
5. Devred, A., General formula for the adiabatic propagation velocity of the normal zone. IEEE Transaction on Magnetics, 1989, **MAG-25 No. 2**, 1968.
6. Scherer M., and Turowski, P., Investigation of the propagation velocity of a normal-conducting zone in technical superconductors. Cryogenics, 1978, **15**, 515.
7. Hirabayashi, H., Morimoto, K., Make, M., Yamada, R., Yamamoto, A., Mori, S., Yoshizaki, R., Kawakami, H., Kondo, K., Aihara, K., Kazawa, Y., Kimura, H., Ogata, H., Saito, R., Suzuki, S., and Miyake, Y., Measurement of propagation velocities of the normal zone in a 1mϕ×1m superconducting solenoid magnet. Jpn. J. Appl. Phys., 1981, **20**, 2243.
8. Lottin, J. Cl., private communication.
9. Rubin, L. G. and Brandt, B. L., Letter to the editor on low-temperature thermometry in high magnetic field. Cryogenics, 1987, **27**, 269.